Seismic Performance Evaluation of RCC Hospital Buildings in Pokhara

Sudip Ranabhat [1], Dinesh Kumar Gupta[1]*, Shreedhar Khakurel[1]
[1]Department of Civil Engineering, Pashchimanchal Campus, Institute of Engineering, Tribhuvan University, Pokhara, Nepal
*replydinesh@ioe.edu.np
(Manuscript Received: 12th January, 2026; Revised: 3rd April, 2026; Accepted: 5th April, 2026)

Abstract

Hospitals are the critical infrastructures that must remain operational during and after the seismic events. Pokhara is located in the high seismic zone and faces significant earthquake risk, which impose threat to safety and strength of the hospital buildings. Despite their importance, existing research lacks the study on seismic performance with special focus on Reinforced Cement Concrete (RCC) hospital buildings in Pokhara. This study addresses this gap by evaluating the Seismic Performance of RCC Hospital buildings using Incremental Dynamic Analysis (IDA) and Fragility Analysis. Two RCC framed structures, Block A (without shear wall) and Block B (with shear wall at lift core) were modelled in ETABS V21 and subjected to six representative ground motions to perform Non-Linear Time History Analysis (NLTHA). Seismic Performance were evaluated in-terms of Inter-Story Drift Ratio (IDR), with Peak Ground Acceleration (PGA) serving as Intensity Measure (IM). Finally, IDA curves were generated and fragility curves were developed based on HAZUS-defined drift limits for four damage states. Results indicate that Block A exhibited higher IDR demands (upto 5.7%) compared to Block B (upto 3.27%) for PGA upto 2g. For 0.35g PGA, Block A showed IDR of 1.4% while Block B demonstrated IDR of 0.57%. Fragility analysis revealed Block A had less than 0.3% probability of collapse, while Block B demonstrated resilience by reaching only lower damage states at 0.35g. For 0.35g PGA, Block A displayed 99% and 9% probability of exceeding Moderate and Extensive Damage State respectively. Similarly, for Block B at 0.35g, there is 99% and 3% probability of exceeding Slight and Moderate Damage State respectively. IDA and Fragility analysis of the building showed that the building remains in an operational state after Maximum Considered Earthquake level ground motions, requiring only minor non-structural repairs.

Keywords: Fragility Curve, Flexural Stiffness, Inter-Story Drift Ratio, Incremental Dynamic Analysis, Performance Evaluation, RCC Hospital Buildings

1. Introduction

Nepal is one of the world's most earthquake prone countries, and has experienced large number of devastating earthquakes of magnitude more than 7.5 Richter Scale (Ram & Wang, 2013). Some of the greatest magnitude earthquakes in Nepal were experienced in the year 1255 AD, 1810 AD, 1866 AD, 1934 AD, 1980 AD, 1988 AD and 2015 AD. 1934 AD earthquake of magnitude 8.4 Richter Scale was experienced to be one of the most devastating earthquakes in the history with a loss of more than 80,000 buildings and 8,500 human lives (WHO). In 2015, Nepal experienced two major earthquakes of 7.8 RS on April 25 and 7.3 RS on May 12, which claimed about 9,000 casualties and 22,300 injuries. About 8 million people (one-third of the national population) were directly affected, and over half a million houses collapsed. The gross domestic product (GDP) dropped by over 1.5 percentage points (NPC, 2015).

Due to 2015 Earthquake, total of 446 public health facilities and 16 private facilities were completely destroyed and, 765 health facilities or administrative structures were partially damaged (NPC, 2015). Because of their vital role in providing medical care both during and after disasters,

hospitals and other healthcare facilities are emphasized by the World Health Organization as critical infrastructure. Also, Nepal National Building Code (NBC 105:2020) has classified Nepal as a region with seismic zone V, which indicates earthquakes are very much active in these regions. In such an environment, critically important facilities like hospitals must maintain structural integrity and functionality after earthquakes. The role hospitals play in an effective community disaster response has been increasingly recognized (Cristian, 2018; Zhong et al., 2014), and resilient hospitals have become central in global disaster risk reduction initiatives. For example, the more recent Sendai Framework for Disaster Risk Reduction 2015 - 2030 (2017) calls for resilient national health systems and critical infrastructures, and has outlined the procedures required to lower disaster risks in a number of sectors, including the health sector.

Destructive earthquakes are uncommon in comparison to other natural disasters, but they can have disastrous effects on communities, possibly causing a disproportionate number of fatalities, injuries, and homeless people as well as long-term effects on the social and economic life of large areas (Gaetani d'Aragona et al., 2024). Because of this, probabilities of the seismic hazard increase which is un-desirable. Melani et al. (2016) noted that to minimize the probabilities of seismic hazards, Seismic Risk Assessment is very much essential.

Gaetani d'Aragona et al. (2024) highlighted that techniques for assessing the seismic vulnerability of large building stocks generally rely on the adoption of fragility curves expressing the probability of exceeding relevant Damage States (DSs) as a function of a ground motion intensity measure (IM). Kassem et al. (2020) reviewed the methods of Seismic Vulnerability Assessment and noted that to develop vulnerability curves, four distinct methods can be utilized; (a) Expert and judgmental approach (b) empirical, which calibrates the functions based on the damage data from surveys performed in the aftermath of strong seismic events (c) analytical, which defines fragility based on the analysis of structural models simulating the behavior of buildings, and (d) hybrid methods, which combine analytical and empirical data.

Budthapa et al., (2024) carried out IDA to access the seismic fragility of multi-story building in Site Class D with mass irregularity, concluding that building with higher mass irregularity at higher levels are more susceptible the earthquake damage. Ghimire & Chaulagain, (2020) conducted seismic fragility assessment of institutional building of Pokhara University using NLTHA and plotted the fragility curve at different damage states. Dawadi & Thapa, (2021) generated the fragility curve of Matepani Gompa in Pokhara and concluded to strengthen the building to increase the safety of the building. K. Ghimire & Ranabhat, (2025) compared the analysis of RCC Apartment Building designed in Site Class B as per NBC 105:2020 with the different prevailing codes. The existing literature omits the study of RCC Hospital Buildings, which are critical infrastructures, in the Site Class B and seismic zone factor of 0.35, where earthquakes are active.

This study considers two building blocks with the objective of determining the performance of the RCC Hospital buildings under seismic action. Kassem et al. (2020) noted that IDA (which is an analytical approach) provided a clear picture of how a structure would behave in the event of seismic activity, and it helps in the development of the fragility curve. This IDA has been carried out in the ETABS software, using the NLTHA method of structural analysis as used by various researchers (Bhandari et al., 2022; Fauzan et al., 2025; Folić & Čokić, 2021).

2. Methodology

Fig. 1 shows the sequential methodological framework that has been adopted in this study. The study generally starts with the description of the building and Finite Element Modeling. Then the process of ground motion selection to normalization is followed, which is again followed by NLTHA. This continuous process of NLTHA with the varying seismic intensity is the Incremental Dynamic

Analysis, which helps in obtaining IDR's and the IDA curve. Based on the developed IDA curve and the drift limit value from HAZUS, fragility curve of both the building blocks in both the direction is generated.

2.1 Incremental Dynamic Analysis

As per Palsanawala et al. (2024), sophisticated nonlinear dynamic analysis method for conducting a thorough evaluation of the lateral behavior of structures under real-world ground motion conditions is incremental dynamic analysis, or IDA. As part of IDA, the structural model is assessed using nonlinear dynamics under a range of ground motion data with different levels of seismic intensity. Usually, peak ground acceleration (PGA), spectral displacement (SD), and peak ground velocity (PGV) plotted against the structural response serve as indicators of seismic intensity (Porter, 2021). Individual peak storey drifts, peak floor accelerations, and inter-storey drift-all of which are measured by an engineering demand parameter (EDP)-can be displayed as an IDA curve for every ground motion record. In the IDA curve, the mean (μ) and standard deviation (σ) of IM (Y-axis) at different value of IDR (X-axis) can be determined, which is used to develop fragility curve.

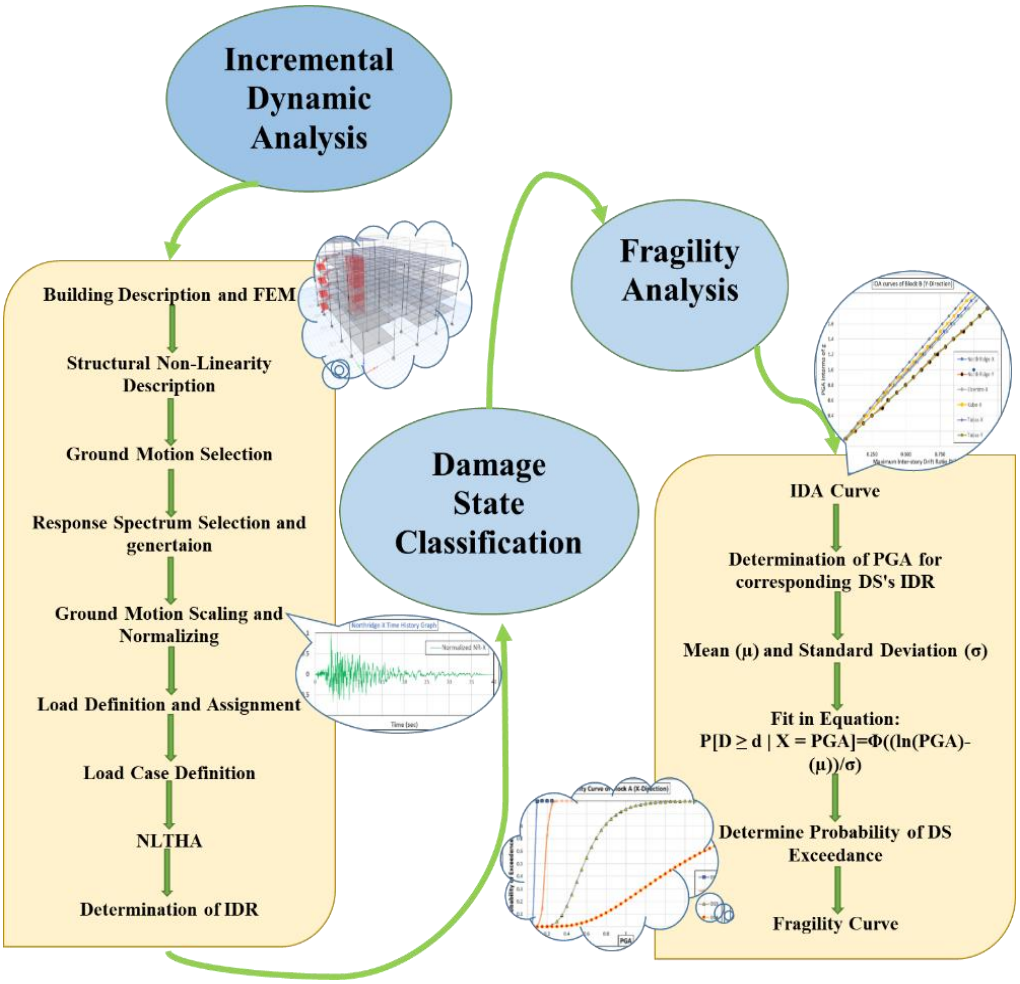

Fig. 1: Methodological Flowchart

2.1.1 Building Description and Modelling

The buildings considered in this study are the existing RCC Hospital Buildings located in Pokhara, whose cross-section details are shown in Fig. 2 to Fig. 4. 3-D Finite Element Models have been developed in the ETABS V21 software, which is one of the most sophisticated software for the modeling and analysis of the buildings. A detailed procedure has been carried out following the CSI

guidelines. The buildings that are being considered for the study are both Special Moment Resisting Frames (SMRF) (NBC 105:2020), with a building height of 18 meters (3.6 meters floor height) with Staircase Cover and a varying bay width from 5m-6.5m. One of the buildings consist of shear wall at lift core. Due to the complications of deriving the field data regarding the strength of the structural members, the strength of concrete and rebar are taken as the design strength, with 25 MPa as the compressive strength of concrete and 500 MPa as ultimate strength of rebar. Member flexural stiffness for beam is considered as 0.35EI (NBC 105:2020; ASCE 41: 2013) and for columns, flexural stiffness is considered as per codal provision (ASCE 41, 2013) to capture non-linearity in the structure. The value of the flexural stiffness modification factor ranges between 0.7 (for axial force greater than or equal to 0.5AgFc) and 0.3 (for axial force less than or equal to 0.1AgFc). For axial forces between these values, the flexural modification factor is calculated using interpolation. The axial force in the column is found between 20.6 KN to 4227.5 KN from the modal analysis. Hence, for building Block A, flexural modification factor lies between 0.3-0.67, whereas for block B, its value ranges between 0.3-0.472. Other definitions include the mass source, restraints, diaphragms, etc. For the purpose of defining mass source, clause 5.2 of NBC 105:2020 is used and it is as shown in the Table 1.

Table 1: Mass Source Coefficient Definition (NBC 105:2020)

Load Type	**Coefficient used**
All Dead Load	1
Live load	
For storage purpose	0.6
For other purpose	0.3

Modeling of the sub-structure is not carried out for the analysis purposes; hence, fixed support is provided at the plinth level, as shown in the model. All the floors are assigned with diaphragms to create a continuous load path from slab to the soil below sub-structure. Rigid joint factor is taken as 0.5 at connection of all beam-column joint. Fig. 2 shows the existing column-beam layout plan, and Fig. 3 shows cross-sectional details of all the columns and beams that currently exist on the building, whose sizes are verified in the field. The final model created is shown in the Fig. 4 and Fig. 5.

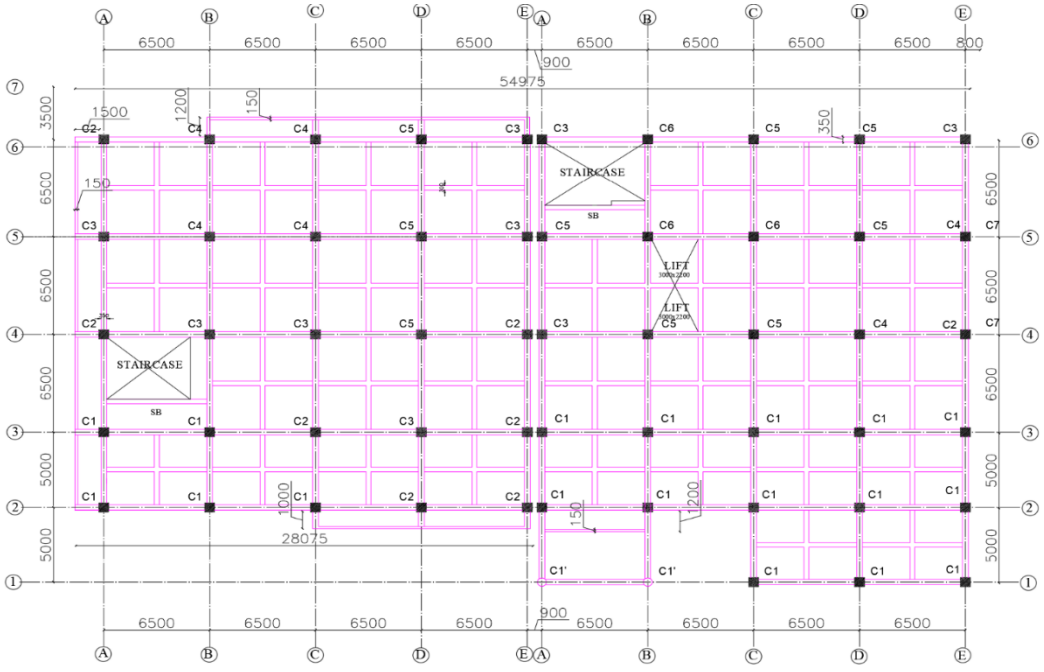

Fig. 2: Beam and Column Layout Plan: Block A (Left) and Block B (Right)

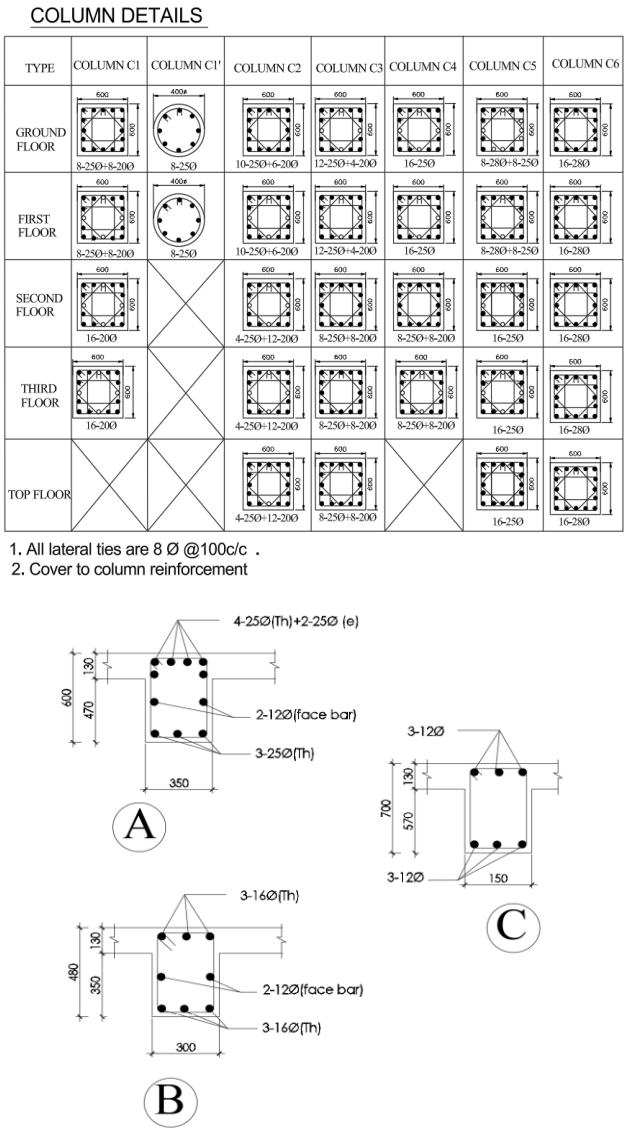

Fig. 3: Cross-section of: Column (Left) and A. Main Beam, B. Secondary Beam, C. Show Beam (Right)

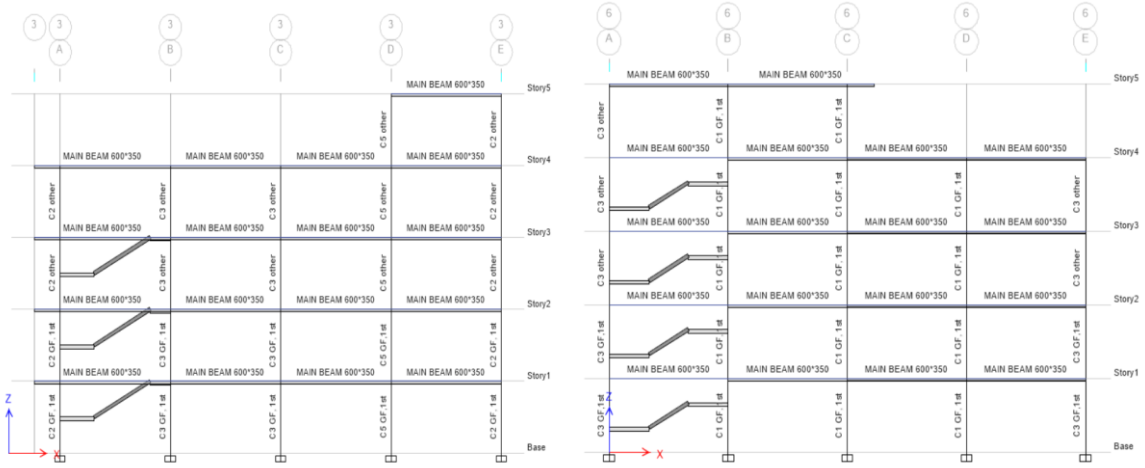

Fig. 4: Sectional View of: Block A (left), Block B (Right)

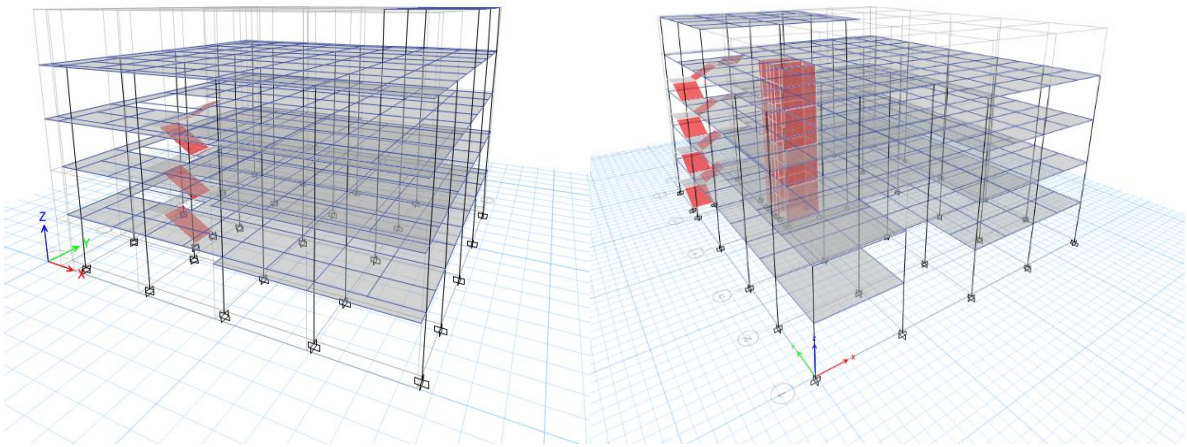

Fig. 5: ETABS Model of: Block A (Left), Block B (Right)

2.1.2 Structural Non-Linearity Definition

Non-linearity is mainly defined by the Geometric and Material Non-Linearity. To define the Geometric Non-linearity, P-delta effect has been defined in the model. Material non-linearity has been assigned to material properties as well as member section properties. To define non-linearity in concrete, hysteresis type is selected as concrete with 50% degradation factor and stress-strain curve given by Mander is used. The non-linearity of the hinges is highly affected by the amount of reinforcement assigned in each structural member. For defining non-linearity in rebar, hysteresis type is selected as Kinematic and other values are kept as default.

Also, the material non-linearity is defined through the use of hinges, which are regions that release the moment from structural members. Hinges generally form at a distance of h/2 from end of member, where h is the depth of member. To account for this, auto hinge is defined at a relative distance of 0.05 *length of member and 0.95* length of member for beams. In the case of column, P-M2-M3 hinges are defined and for shear wall, fiber hinges are defined. ETABS provides the option to define the non-linear auto hinges according to table 41-13 of ASCE.

2.1.3 Ground Motion Selection

As per FEMA P-695 (2009), ground motion record sets include a set of ground motions recorded sets at sites located greater than or equal to 10 km from fault rupture, referred to as the ‘Far-Field” record set, and a set of ground motions recorded at sites lee than 10 km from fault rupture, referred to as the “Near-Field” record set. A selected ground motion should be such that it is consistent with the requirement of the codes, it represents very strong ground motion, it can statically represent large number of records, dependent to each type of the structure as well as the site where the structure is located. No single set of records can fully meet all of these criteria. Large magnitude events are rare, and few existing earthquakes ground motion records are strong enough to collapse large fractions of modern, code-compliant buildings. Hence a sufficient number of ground motions shall be taken so that they can address the above-mentioned criteria. Clause 9.3.2.2 of NBC 105:2020 requires a minimum of three ground records so that it fulfills the above mentioned criteria. Hence, for this study six ground motion data base have been considered.

Because of the composition of over 3,550 ground motion recordings that represent over 160 seismic events (including aftershock events) ranging in magnitude from M4.2 to M7.9, the PEER NGA database was chosen for use in this study for several reasons, including the large number of ground motion records, and the availability of fault-normal and fault-oblique components of ground motion (Lai et al., 2015). When the PEER ground motion database is used for searching the ground motions, the selection of the ground motion is affected by various factors, where location of the structure is more

dominant. For our building located in Pokhara with seismic zone factor 0.35, the following (Table 2) selection criteria are adopted. The procedure for the ground motion selection and scaling has been followed as per FEMA P-695 (2009).

Table 2: Ground Motion Selection Parameters (PEER)

S.N	Parameters	Adopted Value	Range	Reference
1	Fault Type	Reverse/oblique		
2	Magnitude	6, 8.4	>6	Maximum and Minimum considered earthquake in history of Nepal
3	R_JB (km)	0, 30		
4	R_rup (km)	30, 100		
5	Vs30	180, 720	>150	USGS slope based mosaic, hazard study
6	D5-95 (s)	10, 40	5-40	
7	Max. Records No	22	<100	FEMA P-695 (2009)

A sufficient number of the ground motions are selected and among these ground motions, only six are selected to fulfill the minimum criteria as prescribed by various codes and standards. The considered ground motions are Kobe-X, El Centro-X, Tabas-X, Tabas-Y, Northridge-X and Northridge-Y.

Dawadi & Thapa (2021) concluded that variations in the peak amplitude and duration of the ground motions creates variations in the response of the structure. FEMA P-695 (2009) suggests that the selected ground motions should be such that it should produce unique effect on the structure. Table 3 shows different ground motions with different response spectrum (Fig. 8), PGA and duration that are selected for performing Non-Linear Time History Analysis of the corresponding buildings.

2.1.4 Response Spectrum Selection and Generation

The selection of the response spectrum is a critical step in carrying out the performance-based design of the structure, as it ensures that the input ground motions used in the analysis are representative of the seismic hazards at the site. The response spectrum curve is selected from NBC 105:2020 conforming to the site condition of Pokhara. Clause 4.1.2 of the code gives the criteria for the selection of the curve in the form of spectral shape factor (Ch(T)) (Fig. 6). Following the site condition of Pokhara with soil type B, Ta is taken as 0.1, Tc as 0.7, α as 2.5 and K as 1.8 (NBC 105:2020).

For this curve to be used in the Non-Linear Time History Analysis, it needs to be converted into the Response Spectrum Curve (Fig. 6), and it has been done as per the clause 9.3.2.2 of NBC 105:2020. This clause requires the obtained Ch(T) values to be multiplied by seismic zoning factor (z), importance factor (I), and divided by over strength factor (Ωu). Considering the MCE level of earthquake, the z value is 0.35 for Pokhara, and for hospital building, the I value is taken as 1.5. Over strength factor is taken as 1.5 as prescribed by the code. The generated Ch(T) curve and response spectrum curve is shown in the Fig. 6.

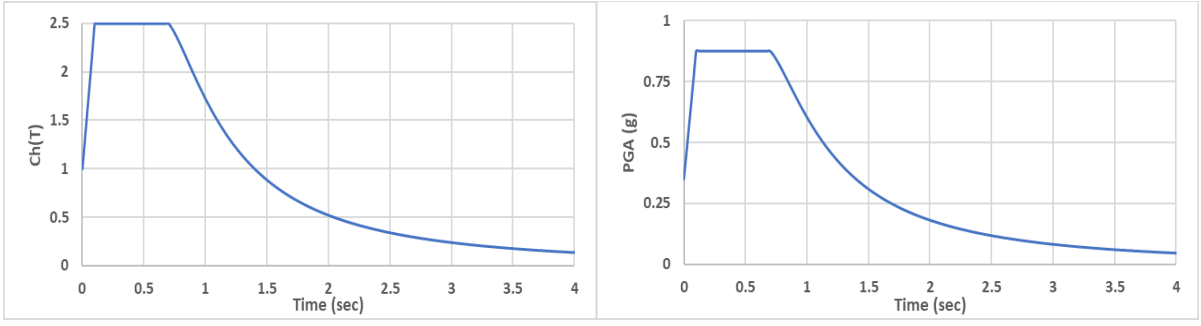

Fig. 6: Spectral Shape Factor Curve (Left), Response Spectrum Curve (Right)

2.1.5 Ground Motion Scaling and Normalization

To adjust the property of the ground motion as per the site location, it is important to carry out spectral matching. This is achieved out with the help of software named Seismo-Match. Spectral matching is done for a damping ratio of 5% between the time interval of 0.05 sec to 4 seconds, using the response spectrum as shown by Fig. 6. In-order to apply the load to an increasing intensity, it is important to normalize the matched ground motions by using a suitable scale factor. For the Northridge-X case, the matched PGA is 0.5128 g and hence the scale factor is 1/0.5128=1.95. The Fig. 7 below shows the comparative visualization of all the ground motion's Original, Matched and Normalized Time History Records.

The Target Spectrum shown in Fig. 8 is the NBC 105:2020 Response Spectrum curve for Site Class B as displayed in Fig. 6, where all the ground motion's response spectra are observed consistent with this curve. From the 22 records selected from the PEER Database, only 6 ground motions whose Response Spectrum got matched and are consistent with the Target Spectrum were used for the NLTHA. The same procedure is followed by Budthapa et al., (2024).

Table 3: Selected Ground Motions (PEER) and their properties

S.N.	Earthquake name	Station Name	Original PGA	Matched PGA	Normalization Factor	Normalized PGA	Recorded Time Duration
1	Northridge-X	Nordhoff Fire Station	0.3451	0.5128	1.950078	1	60 secs
2	Northridge-Y	Nordhoff Fire Station	0.3078	0.40821	2.44972	1	60 secs
3	Elcentro-X	El Alamo	0.03348	0.41234	2.425183	1	40 secs
4	Kobe-X	Osaj	0.0825	0.4476	2.234138	1	150 secs
5	Tabas-X	Boshrooyeh	0.1033	0.41637	2.40171	1	35 secs
6	Tabas-Y	Boshrooyeh	0.0848	0.3548	2.818489	1	35 secs

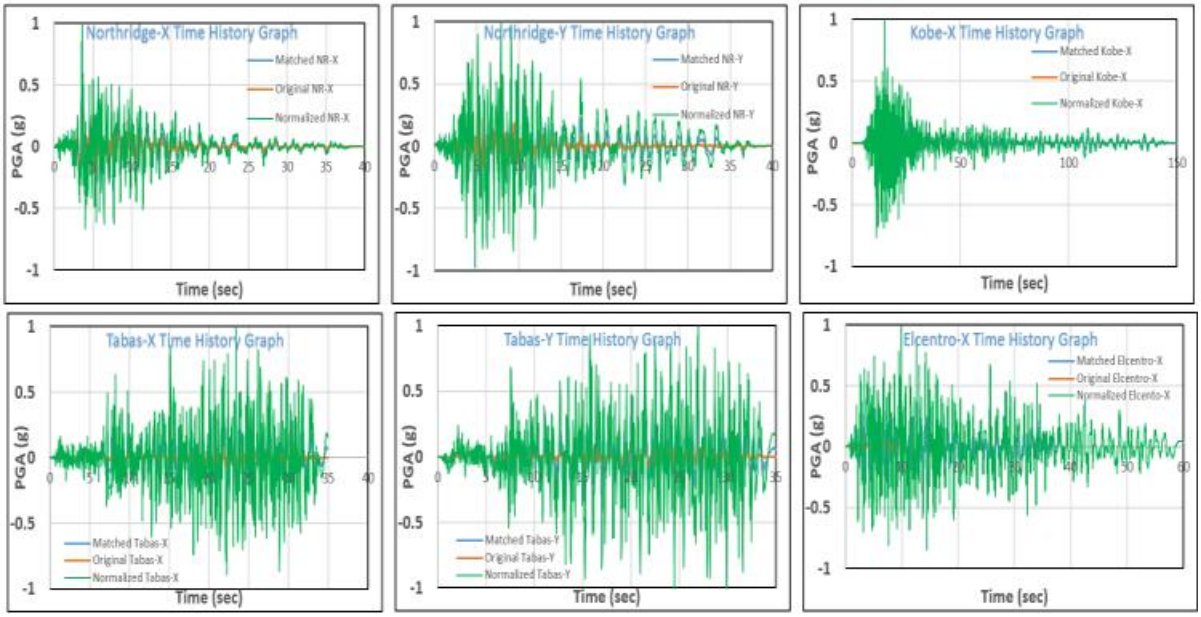

Fig. 7: Comparative Visualization of all Selected Ground Motion's Time History Records

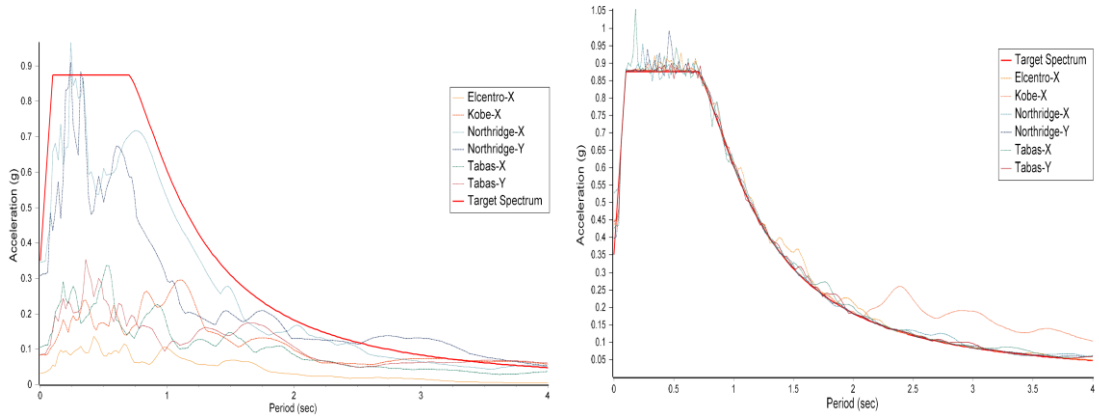

Fig. 8: Response Spectra of Selected Ground Motion's Time History Record Before Spectral Matching (Left) and After Spectral Matching (Right)

2.1.6 Load Definition and assignment

After the modeling and ground motion selection has been completed, the model needs to be loaded with various types of loads such as dead load, live load, earthquake load, etc. Various types of load cases as per the IS 875 Part I (Dead Load) and Part II (Live Load) have been taken. Earthquake load have been taken from the normalized time history records and applied to the model. The applied dead load and live load are shown in the Table 4 and Table 5.

Table 4: Dead Load (IS 875 Part I)

Purpose	Load Calculation	Load Assigned
9" thick wall with no opening considered	3* (0.23 *19.2 + 0.05 * 20.4) =16.308	17 KN/m
9" thick wall with 25% opening considered	16.308* 0.75=12.231	13 KN/m
4" thick wall with no opening considered	3m * (0.1 *19.2 + 0.05 * 20.4) =8.82	9 KN/m
4" thick wall with 25% opening considered	8.82* 0.75=6.615	7 KN/m
Floor Finish Load for balcony, corridors, lobby, staircase	(26.7*0.025+0.05*22.4) = 1.7875	1.8 kN/m^2
Floor Finish Load for rooms, toilet, bathroom	(21*0.01+0.05*22.4) = 1.33	1.4 kN/m^2
Floor Finish for Roof	(0.006*21+0.05*22.4) = 1.246	1.3 kN/m^2
Partition Load	1.5	1.5 kN/m^2

Table 5: Live Load (IS 875 Part II)

Purpose	Minimum LL as per IS 875 part II
Bed rooms, wards, dressing rooms, dormitories and lounges, T/B	2 kN/m^2
Kitchens, laundries and laboratories, dining rooms, cafeterias and restaurants, X-ray rooms, operating rooms, general storage areas	3 kN/m^2
Office rooms and OPD rooms	2.5 kN/m^2
Corridors, passages, balconies, lobbies and staircases including fire escapes -as per the floor serviced	4 kN/m^2
Boiler rooms and plant rooms	5 kN/m^2
Probable Partition	1.5 kN/m^2
Roof Accessible	1.5 kN/m^2
Roof Not Accessible	0.75 kN/m^2

2.1.7 Load Case Definition

For the non-linear time history analysis, the results are highly affected by the load case selected. Initially, the model needs to be run by the non-linear static load case, and then after by the non-linear dynamic case. For the purpose of NLTHA, Fast Non-Linear Analysis method has been selected over the Direct Integration Method because of the fastest computational time as per the reference of CSI manual. For NLTHA, two major load cases are defined. One is the NSC (Non-Linear Static Case) and other is the NDC (Non-Linear Dynamic Case) both as FNA.

2.2 Drift Limit States Classification

Drift Limit States decides the criteria for the collapse of the structure. In this methodology, four damage states: Slight Damage (SD), Moderate Damage (MD), Extensive Damage(ED) and Complete Damage (CD) have been used as defined by HAZUS for generic buildings. These values are very much significant in deciding at what intensity will failure occur in buildings. The classification of the different drift limit states and their reparability according to HAZUS is shown in the Table 6 and Table 7.

Table 6: Drift Limiting Values (HAZUS)

Model Building Types	**SD (DS1)**	**MD (DS2)**	**ED (DS3)**	**CD (DS4)**
C1M (Medium Rise Concrete Frame)	0.33%	0.66%	2%	5.33%
C2M (Medium Rise Shear Wall Frame)	0.26%	0.66%	2%	5.33%

Table 7: Failure modes and reparability of different damage states (HAZUS)

Description	**Failure Conditions**	**Reparability**
Slight Damage (SD)	-Minor cracks in walls, ceilings, or floors. -No visible damage to the building's main structural parts. -Some nonstructural items like ceiling tiles or windows may be slightly affected.	-Building is safe to occupy. -Repairs are simple, such as patching cracks or replacing small items.
Moderate Damage (MD)	-Larger cracks in walls or floors. -Some bending or minor damage to structural elements like beams or columns. -Nonstructural systems like pipes or light fixtures may be damaged.	-Building may need to be closed temporarily. -Repairs require professional help but the structure can be fixed.
Extensive Damage (ED)	-Serious damage to structural parts such as broken beams, cracked columns, or shifted walls. -Many nonstructural systems are also damaged.	-Building may be unsafe to enter. -Repairs are difficult and costly. -Some parts may need to be rebuilt.
Complete Damage (CD)	-Major parts of the building have collapsed or are close to collapsing. -Structural systems have failed. -Most systems in the building are destroyed.	-Building is not repairable. -It is considered a total loss and must be demolished and rebuilt.

2.3 Fragility Analysis

As per Porter (2021), fragility functions are more generally defined as mathematical functions that express the likelihood of an undesirable event occurring as a function of some measure of environmental excitation. There are many equations to plot the seismic fragility curve, however the $Equation$ 1 has

already been used by many researchers Kassem et al. (2020a), Ibrahim & El-Shami (2011) and hence it is used in this study.

$$F\_dx = P[D \geq d \mid X = x] = \Phi\left(\frac{lnln(x) - (\mu_d)}{\beta_d}\right) \quad (1)$$

Where,

- Φ (·)= Standard normal cumulative distribution function
- ln(x) = Natural logarithm of the demand level x
- μ_d= Mean demand value at which damage state d is reached (in log scale)
- β_d= Logarithmic standard deviation (dispersion) for damage state d

This Equation shows that, fragility function is dependent on the value of x (Intensity Measure), and μ, β which are again dependent on IM, Ground Motion Data and EDP. By taking the value of μ and σ as constant and varying the value of x, the fragility curve which gives the probability of exceedance of damage states can be determined and plotted.

2.3.1 Mean value and Standard Deviation of Intensity Measure: PGA

Corresponding to the limit value of different damage states, mean(μ) and standard deviation (σ) of PGA have been calculated for the different sets of ground motions.

$$Mean\ (\mu) = \frac{Sum\ of\ lnln\ (IM)\ of\ all\ GMS\ (\sum x)}{Total\ number\ of\ Ground\ Motions\ (n)} \quad (2)$$

$$Standard\ Deviation\ (\sigma) = \sqrt{\sum (ln\ ln\ (IM)\ - \mu)/(n-1)} \quad (3)$$

2.3.2 Development of Fragility Curve

If PGA is taken as IM or x and mean and standard deviation are denoted as μ and σ respectively, then the equation given in the $Equation$ 1 can be updated as:

$$P\left(\frac{D}{PGA}\right) = \emptyset\,\frac{(lnln\ (PGA) - \mu)}{\sigma} \quad = \quad f(x) \quad (4)$$

To draw the fragility curve, the obtained value of mean(μ) and standard deviation (σ) from Equation 2 and 3 has been used in Equation 4.

The elaborated form of the above equation is:

$$f(x) = \frac{1}{x\sigma\sqrt{2\pi}} \exp\left(-\frac{(\ln x - \mu)^2}{2\sigma^2}\right), \quad x > 0 \quad (5)$$

3. Results and Discussion

3.1 Results of Incremental Dynamic Analysis

IDA is a procedure used to predict the collapse capacity of the various structures under earthquake records with different characteristics and intensities. Each of the building models were analyzed with different intensities in the interval of 0.1 till the collapse occurs or up to 2g, which is achieved earlier i.e. analysis stoppage point = earliest (5.33% IDR, 2g PGA). It is done so because of the largest computational time of the IDA using NLTHA.

3.1.1 IDA of Block A

The result that is obtained after IDA is extracted in-terms of EDP, where IDR is considered as EDP in this study. When NLTHA is carried out for multiple times with an increasing intensity of the earthquake load or any dynamic load and during each time, IDR is noted, then it becomes the part of IDA. The IDA curves of Block A as shown in Fig. illustrate how the structure responds to increasing seismic intensity by plotting Peak Ground Acceleration (PGA) against maximum inter-story drift ratio (%) for six different ground motions. From the Fig. 9, it can be seen that with increase in intensity, there is increase in the inter story drift ratio. Also, we can observe that the variation of IDR with the PGA is

linear. It is due to the use of FNA method over the DI method and the same nature of the curve is developed by Budthapa et al., (2024).

It indicates that increase in intensity of earthquake increases the chances of achieving damage states. Using the HAZUS-defined drift limit states: Slight Damage (0.33%), Moderate Damage (0.66%), Severe Damage (2.0%), and Complete Damage (5.33%), we can evaluate the performance of the structure under each earthquake record. At 0.33% drift (SD), all motions have PGA under 0.104g, showing minimal damage from minor seismic excitations. At 0.66% drift, PGA ranges from 0.15g–0.21g, indicating minor yielding begins in certain structural elements. At the severe damage threshold of 2.0% drift, IDA curves show greater variation; Elcentro-X and Tabas-Y cause damage near 0.5g, while Kobe-X requires about 0.7g PGA. At the complete damage state (5.33%), Kobe-X in particular-reach or approach this level at higher PGAs nearing 1.8g to 2.0g. The same value of drift is achieved by Tabas-Y at just about 1.3g, indicating the more vulnerable earthquake in these suites of selected GMs.

The IDA curve for Block A in Y-direction show a similar trend to the X-direction (Fig. 9), but the response is more uniform than the X-direction suggesting potentially better lateral stiffness or distribution in the Y-direction. This trend agrees with the findings from Vamvatsikos & Cornell (2002), reinforcing the impact of ground motion variability and the utility of IDA in capturing structural fragility across directions.

3.1.2 IDA of Block B

The IDA curve of Block B is shown in Fig. 10. Because of the presence of shear wall around lift core, the HAZUS-defined drift limit state for Slight Damage is 0.26% while the other criteria remain same. The IDA curve reveals that, for all the ground motions, the obtained IDR values are very low rarely exceeding the moderate damage state at strong magnitude of about 1.2g. This is due to the fact of the presence of shear wall around lift core, which largely increases the stiffness of the building. This increase in stiffness decreases the lateral displacement, which is directly related to the inter-story drift and the ratio. This is echoed by Aslani & Tehrani, (2025); Kassem et al., (2020a) that the addition of shear walls in building increases the performance of the buildings by reducing the considered response measuring parameter i.e. IDR. Because of this reason, this building block barely experiences severe and complete damage states for the considered earthquakes of magnitude up to 2g. Also in the Y-direction, the values are nearly same as that of the X-direction with very much minor differences which can be neglected. Hence, we can predict that the building in both X- and Y-direction can effectively resist larger magnitude earthquake events.

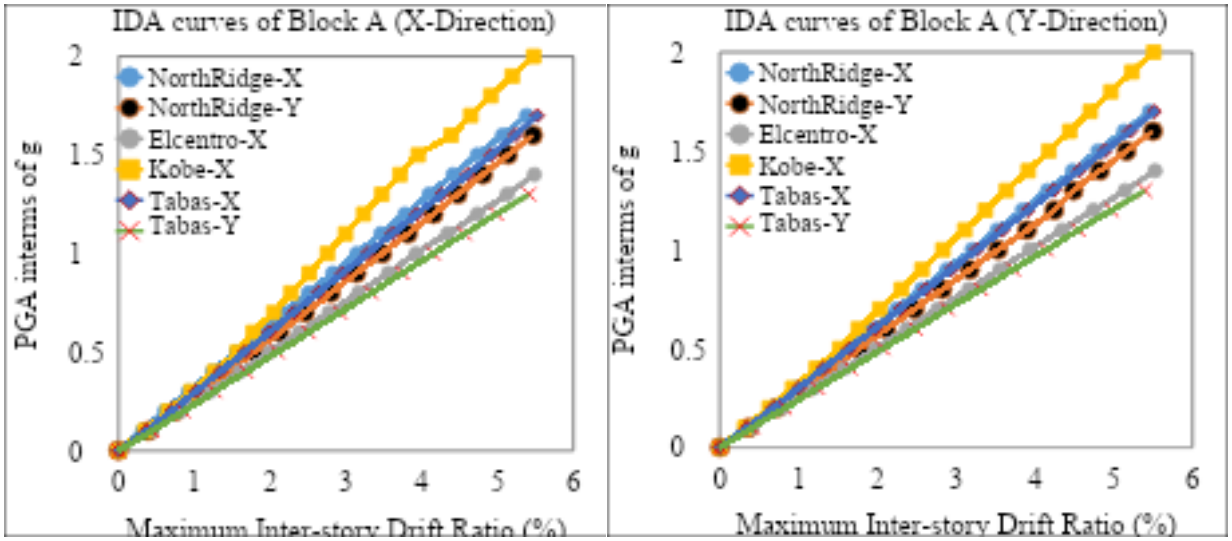

Fig. 9: IDA curve of Block A X-direction (Left) and Y-direction (Right)

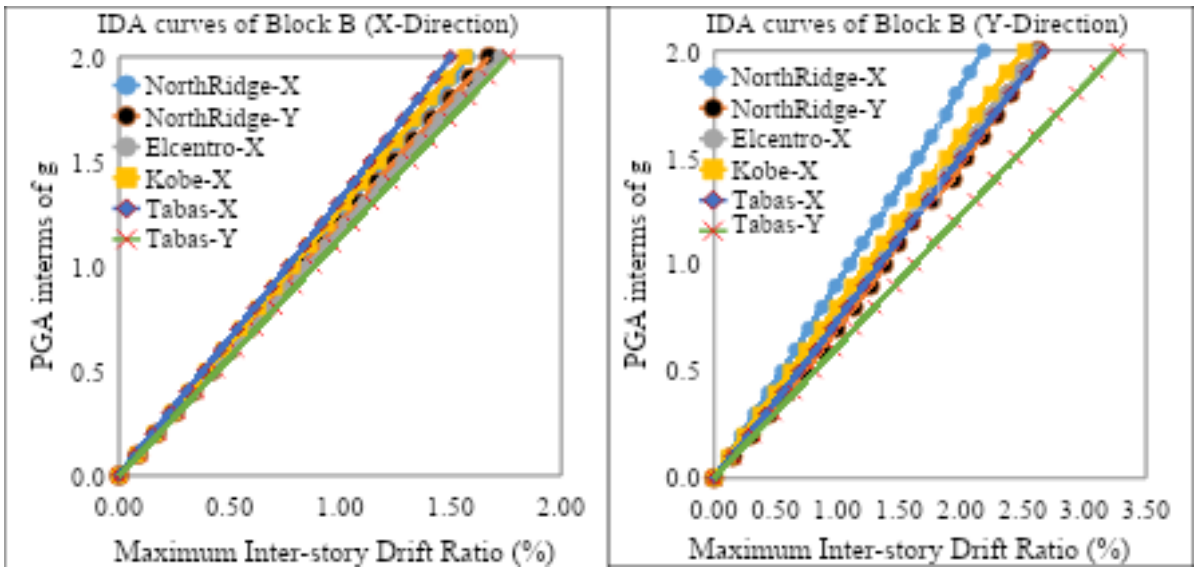

Fig. 10: IDA curve of Block B X-direction (Left) and Y-direction (Right)

3.2 Fragility Analysis

After plotting the IDA curves, the corresponding PGA for the different damage states were determined for different records. Using these IDA data, fragility curves can be developed to represent the probability of structure reaching or exceeding specific damage states under varying levels of seismic intensity (Aslani & Tehrani, 2025). These curves are essential for assessing the vulnerability of structures to earthquakes. Subsequently, a Cumulative Distribution Function (CDF) was applied to the data sets to determine the collapse probabilities at different PGA levels and the fragility curves for the structures in X and Y direction have been plotted. The cumulative distribution function follows the form as shown in the equation below based on the assumption of lognormal distribution.

$$P[D \geq d \mid X = PGA] = \Phi\left(\frac{ln(PGA) - (\mu)}{\sigma}\right) Mean\ (\mu) = \frac{Sum\ of\ ln\ ln\ (IM)\ of\ all\ GMS\ (\sum x)}{Total\ number\ of\ Ground\ Motions\ (n)}$$

$$Standard\ Deviation\ (\sigma) = \sqrt{\sum (ln\ ln\ (IM)\ - \mu)/(n-1)}$$

$$f(x) = \frac{1}{x\sigma\sqrt{2\pi}} \exp\left(-\frac{(\ln x - \mu)^2}{2\sigma^2}\right), \quad x > 0$$

Calculation Example for DS1 at PGA=0.1g:

Mean (μ)=(-2.26-2.48-2.561-2.35-2.414-2.604)/6=-2.445

For NR-X, $(\ln(IM)-\mu)^2$= $(-2.26+2.445)^2$=0.012

$\sum(\ln(IM)-\mu)^2$=0.034

Standard Deviation (σ)=√(0.031/5)=0.049

For PGA=x=0.1,

$$P[D \geq d \mid X = 0.1] = \Phi\left(\frac{ln\ ln\ (0.1)\ - (-2.445)}{0.0782}\right) = \left\{\frac{exp\ exp\left(-\frac{\left(ln(0.1) - (-2.445)\right)^2}{2 * 0.049^2}\right)}{0.1 * 0.049 * \sqrt{(2 * 3.1428)}}\right\}$$

$$= 0.99 = 99\%$$

3.2.1 Fragility Curve of Block A

The fragility curves in the Fig. 11 show the probability of exceedance for different damage states (DS1 to DS4) of Block A in the X-direction, as a function of Peak Ground Acceleration (PGA). This curve (Fig. 11) shows that there is 100% probability of achieving Slight Damage (DS1) when PGA reaches 0.15g. Approximately at 0.3g, 100% probability of achieving the Moderate Damage (DS2) is observed. When PGA is approximately 1.4g, there is 99% chances of achieving the Extensive Damage (DS3). It is also observed that up to the analyzed intensity of Ground Motions (2g), only 67.5% probability of Collapse Damage (DS4) is observed. For the Block-A in Y-direction, Fig. 11 (right) shows that there is 100% probability of achieving Slight Damage (DS1) when PGA reaches 0.15g. Approximately at 0.3g, 99% probability of achieving the Moderate Damage (DS2) is observed. When PGA is approximately 1.35g, there is 99% chances of achieving the Extensive Damage (DS3). It is also observed that up to the analyzed intensity of Ground Motions (2g), only 68.2% probability of Complete Damage (DS4) is observed.

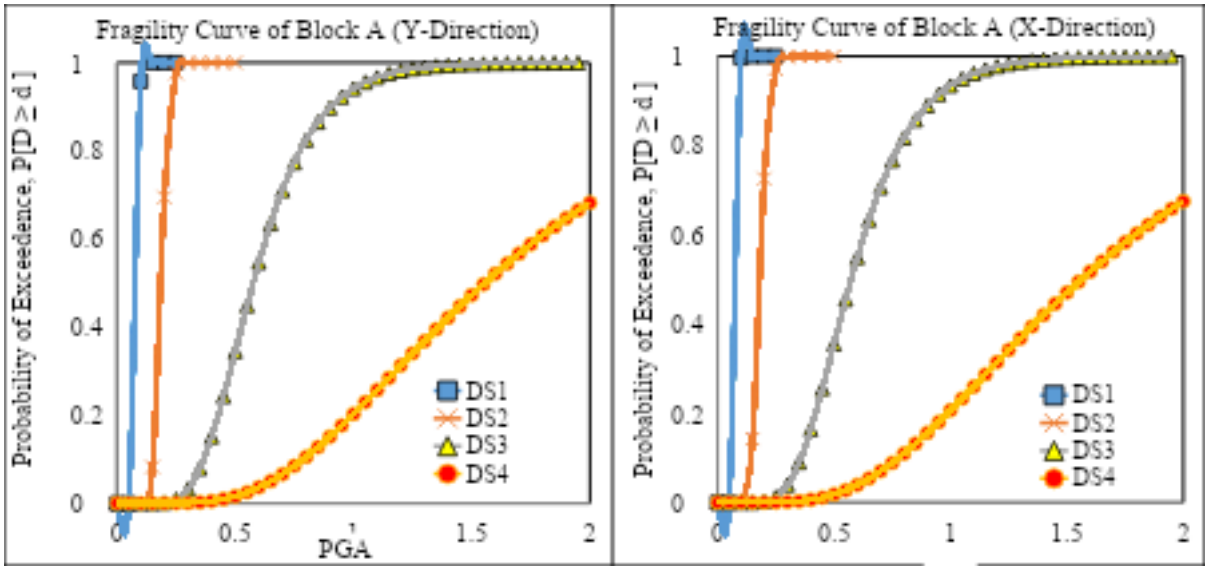

Fig. 11: Fragility curve of Block A X-direction (Left) and Y-direction (Right)

3.2.2 Fragility Curve of Block B

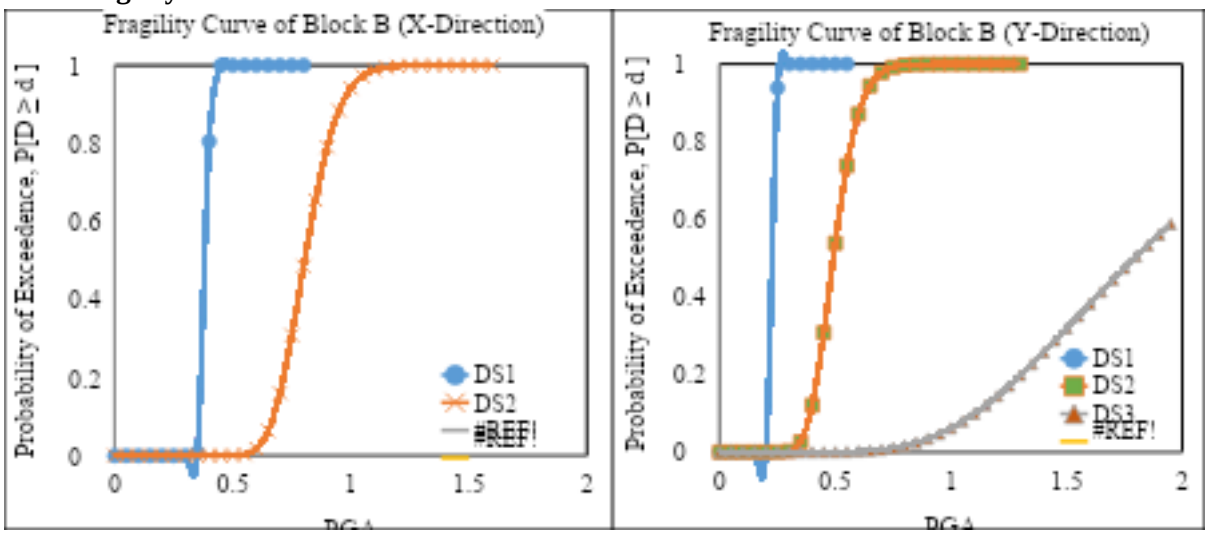

Fig. 12: Fragility curve of Block B X-direction (Left) and Y-direction (Right)

Fig. 12 (left) shows the fragility curve of block B in X-direction, which displays only DS1 and DS2. For the considered PGA up to 2g, IDR of building never exceeded more than 1.763%. This is

because of the greater stiffness of the building due to the presence of shear wall. Hence, the building achieved only DS1 and DS2 for PGA up to 2g. The building will exceed 100% DS1, when PGA is about 0.45g and DS2, when PGA is around 1.2g. Fig. 12 (right) shows the fragility curve of Block B in Y-direction, with the curve of DS1, DS2 and DS3 in it. DS4 curve cannot be generated because IDR of the building never exceeded 3.27% for PGA up to 2g. The building will achieve 100% probability of exceedance of DS1 for PGA of 0.3g, and DS2 for PGA of 0.75g. At PGA of 2g, there will be approximately 60% probability of exceedance of DS3.

The comparative Fig. to illustrate the fragility of RCC Hospital Buildings is shown in Fig. 13. Fig. 13 shows that the buildings are more likely to exceed Slight Damage State with very low probability of achieving Collapse Damage State if they experience seismic events of PGA 0.35g.

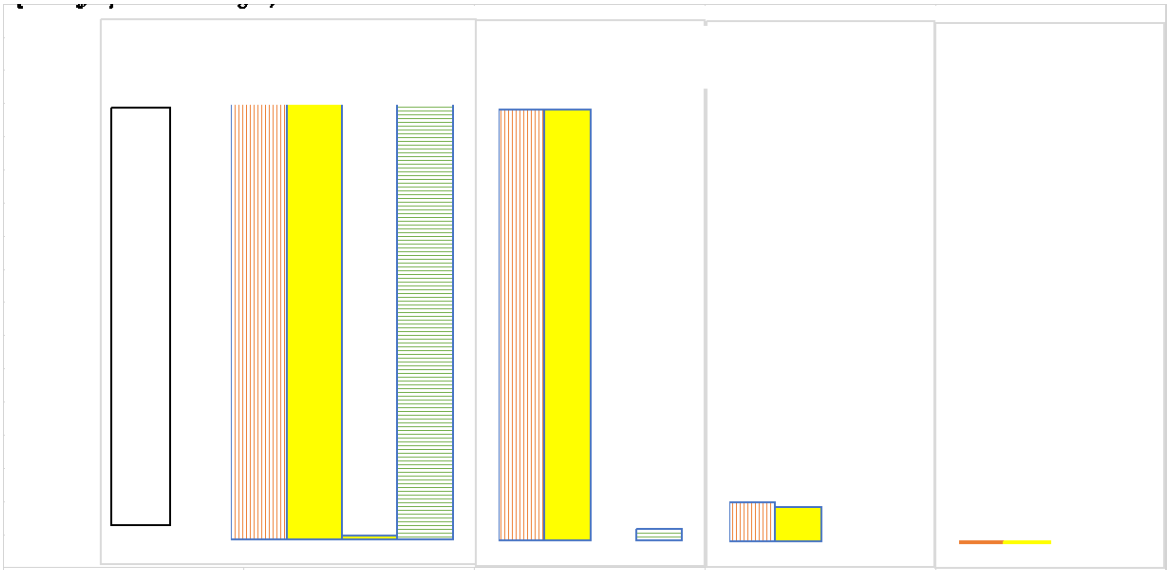

Building	Slight Damage (P [S/ Sd])	Moderate Damage (P [M/ Sd])	Extensive Damage (P [E/ Sd])	Complete Damage (P [C/ Sd])
Block A (X-Direction)	100	99	9	0.3
Block A (Y-Direction)	100	99	7.9	0.24
Block B (X-Direction)	0.75	-	-	-
Block B (Y-Direction)	100	2.67	-	-

Fig. 13: Comparison of Fragility Curves of Block-A and Block-B for PGA of 0.35g

4. Conclusion

This study attempts to carry-out the seismic fragility assessment of RCC hospital buildings in Pokhara, from where the following conclusions have been withdrawn:

- All the ground motions, though they were matched to same response spectrum displayed different values of the IDR. This shows that the response of the structure is dependent on the nature of the time history records of different ground motions.
- EDP (IDR) is highly dependent on the stiffness property of the structural members of the building, which is mandatory for the non-linear analysis of the structure.
- Building Block A showed higher sensitivity to IDR (values ranging from 0-5.7%), whereas Building Block B showed less sensitivity to IDR (IDR ranging from 0-3.27%) for PGA up to 2g.
- In X-direction, Block A achieved DS1, DS2, DS3 and DS4 at 0.074g, 0.152g, 0.476g and 1.28g respectively considering Tabas-Y ground motion which is among the most vulnerable suite of ground motion considered. Similarly, in Y-direction, using same ground motion data, building Block A achieved DS1, DS2, DS3 and DS4 at 0.080g, 0.159g, 0.483g and 1.284g respectively.

▪ For Block B in X-direction, it never achieved DS3 and DS4 for PGA up to 2g, with higher value of 1.763% IDR by Tabas-Y. Similarly, in X-direction, Block B never achieved DS4 for PGA up to 2g, being maximum value of 3.27% IDR in Tabas-Y.

▪ Seismic fragility curves were developed for four damage states (Slight, Moderate, Extensive, and Collapse). The probability of exceeding each damage state increased with increase in PGA.

▪ The Block A structure demonstrated strong resistance to collapse, with less than 0.3% probability of complete failure at 0.35g PGA (MCE level), indicating high seismic resilience. At 0.35g, there is 99%, 99%, 9%, and 0.3% probability of exceedance of Slight, Moderate, Extensive and Collapse damage in X-direction of Block A. Similarly, there is 99%, 99%, 7.9%, and 0.25% probability of exceedance of Slight, Moderate, Extensive and Collapse damage in Y-direction of Block A.

▪ Building Block B has the probability of exceedance of 100% DS1 at PGA of about 0.8g and DS2, when PGA is around 1.9g. This indicates that building has high seismic resilience in X-direction. For the Y-direction also, building has very high seismic resilient capacity with probability of exceedance of 100% DS1 at about 0.7g and DS2 at 1.8g respectively.

▪ Fragility behavior of the building was consistent in both directions for lower damage states; however, the Y-direction showed slightly higher vulnerability at extensive and collapse levels.

To sum up the conclusion, both the building remains in an operational state after MCE-level ground motions, requiring only minor non-structural repairs. Building Block-A seems to be fragile in different scenarios of earthquake but Block B is much resistant to earthquake. During the modeling and analysis, non-structural components (eg., infill walls, medical equipment, partition walls) have not been considered. All the building's structural elements section and material properties have been modeled as specified in the existing structural drawing only i.e. no any modifications have been done on section and property of structural elements. Response spectrum curve as per NBC 105:2020 has been used for spectral matching and drift limiting values are taken directly from the HAZUS manual for Generic Mid-Rise RCC Framed Structure. Other more study can be carried out addressing these limitations on seismic performance evaluation of RCC Hospital Buildings in Pokhara.

Conflicts of Interest

The authors declare no conflict of interest.

References

Aslani, M., & Tehrani, P. (2025). Seismic response and collapse capacity assessment of dual RC buildings with vertical irregularities in shear walls. *Scientific Reports*, 15(1), 9966. https://doi.org/10.1038/s41598-025-94328-z

Bhandari, A., Suwal, R., & Khawas, A. (2022). Seismic Fragility Assessment of Irregular High Rise Buildings using Incremental Dynamic Analysis. *Advances in Engineering and Technology: An International Journal*, 2(01), 69–76.

Budthapa, U., Khawas, A., & Suwal, R. (2024). Seismic Fragility Assessment of Multistory Mass Irregular Buildings using Incremental Dynamic Analysis. J*ournal of Advanced College of Engineering and Management*, 9, 67–77. https://doi.org/10.3126/jacem.v9i1.71427

Cristian, B. (2018). Hospital Resilience: A Recent Concept in Disaster Preparedness. *The Journal of Critical Care Medicine*, 4(3), 81–82. https://doi.org/10.2478/jccm-2018-0016

Dawadi, S., & Thapa, D. (2021). Fragility Analysis of Religious Matepani Gompa in Pokhara. *International Journal of Engineering Research*, 10(09).

Fauzan, F., Agista, G. A., Syandriaji, D., Al Jauhari, Z., & Suwarso, D. B. (2025). Seismic vulnerability assessment of a hospital building with and without retrofitting using RC shear walls. *E3S Web of Conferences*, 604, 15003. https://www.e3s-conferences.org/articles/e3sconf/abs/2025/04/e3sconf_icdm2024_15003/e3sconf_icdm2024_15003.html

FEMA. (2012). Multi-hazard loss estimation methodology HAZUS–MH 2.1 advanced engineering building module (AEBM) technical and user's manual. *Federal Emergency Management Agency*, Washington, D.C.

FEMA P-695. (2009). Quantification of Building Seismic Performance Factors. *Applied Technology Council for the Federal Emergency Management Agency*, Washington, D.C.

Folić, R., & Čokić, M. (2021). Fragility and vulnerability analysis of an RC building with the application of nonlinear analysis. *Buildings*, 11(9), 390.

Gaetani d'Aragona, M., Polese, M., & Prota, A. (2024). Seismic fragility curves for infilled RC building classes considering multiple sources of uncertainty. *Engineering Structures*, 321, 118888. https://doi.org/10.1016/j.engstruct.2024.118888

Ghimire, K., & Ranabhat, S. (2025). A Comparative Study of Middle Rise Apartment Building with Different Seismic Codes. *Pokhara Engineering College Journal*, 2(2), 22–37. (Applied Science and Engineering). https://doi.org/10.3126/pecj.v2i2.81736

Ghimire, N., & Chaulagain, H. (2020). Seismic Fragility Analysis of Institutional Building of Pokhara University. *Himalayan Journal of Applied Science and Engineering*, 1(1), 31–39. https://doi.org/10.3126/hijase.v1i1.33539

Ibrahim, Y. E., & El-Shami, M. M. (2011). Seismic fragility curves for mid-rise reinforced concrete frames in Kingdom of Saudi Arabia. *The IES Journal Part A: Civil & Structural Engineering*, 4(4), 213–223. https://doi.org/10.1080/19373260.2011.609325

Kassem, M. M., Mohamed Nazri, F., & Noroozinejad Farsangi, E. (2020a). On the quantification of collapse margin of a retrofitted university building in Beirut using a probabilistic approach. *Engineering Science and Technology, an International Journal*, 23(2), 373–381. https://doi.org/10.1016/j.jestch.2019.05.003

Kassem, M. M., Mohamed Nazri, F., & Noroozinejad Farsangi, E. (2020b). The seismic vulnerability assessment methodologies: A state-of-the-art review. *Ain Shams Engineering Journal*, 11(4), 849–864. https://doi.org/10.1016/j.asej.2020.04.001

Lai, J., Wang, S., Schoettler, M. J., & Mahin, S. A. (2015). Seismic Evaluation and Retrofit of Existing Tall Buildings in California: Case Study of a 35-Story Steel Moment-Resisting Frame Building in San Francisco, *PEER Report 2015-14*. Pacific Earthquake Engineering Research Center, University of California, Berkeley, CA. https://peer.berkeley.edu/sites/default/files/webpeer-2015-14_jiun-wei_lai_shanshan_wang_matthew_j._schoettler_stephen_a._mahin.pdf

Melani, A., Khare, R. K., Dhakal, R. P., & Mander, J. B. (2016). Seismic risk assessment of low rise RC frame structure. *Structures*, 5, 13–22. https://doi.org/10.1016/j.istruc.2015.07.003

NBC 105. (2020). Seismic design of buildings in Nepal. *Ministry of Urban Development and Building Construction*, Nepal.

NPC. (2015). Nepal Earthquake 2015: Post Disaster Needs Assessment. *National Planning Commission, Government of Nepal*.

Palsanawala, T. N., Gondaliya, K. M., & Vasanwala, S. A. (2024). Seismic fragility comparison of FBD and DDBD designed RC frame using incremental dynamic analysis. *IOP Conference Series: Earth and Environmental Science*, 1326(1), 012006. https://doi.org/10.1088/1755-1315/1326/1/012006

Porter, K. (2021). A Beginner's Guide to Fragility, Vulnerability, and Risk. In M. Beer, I. A. Kougioumtzoglou, E. Patelli, & I. S.-K. Au (Eds.), *Encyclopedia of Earthquake Engineering* (pp. 1–29). Springer Berlin Heidelberg. https://doi.org/10.1007/978-3-642-36197-5_256-1

Ram, T. D., & Wang, G. (2013). Probabilistic seismic hazard analysis in Nepal. *Earthquake Engineering and Engineering Vibration*, 12(4), 577–586. https://doi.org/10.1007/s11803-013-0191-z

UNISDR. (2015). Sendai Framework for Disaster Risk Reduction 2015-2030 (p. 32). *United Nations Office for Disaster Risk Reduction (UNISDR)*. https://www.unisdr.org/we/inform/publications/43291

Vamvatsikos, D., & Cornell, C. A. (2002). Incremental dynamic analysis. *Earthquake Engineering & Structural Dynamics*, 31(3), 491–514. https://doi.org/10.1002/eqe.141

Zhong, S., Clark, M., Hou, X.-Y., Zang, Y.-L., & Fitzgerald, G. (2014). Development of hospital disaster resilience: Conceptual framework and potential measurement. *Emergency Medicine Journal*, 31(11), 930–938.